JOURNAL OF
EMERGING INVESTIGATORS

Article

# Quantifying right atrial dilation relative to atrial septal defect size using an experimental model

**Daniel Lee[1], Grant Trouton[1]**
[1] Oakton High School, Vienna, Virginia

## SUMMARY

**Atrial septal defect (ASD) is a congenital cardiovascular defect in the septum between the heart's upper chambers. Larger ASDs cause significant dilation in the right atrium, which can lead to heart failure and pulmonary hypertension. Current methods poorly predict the severity of right atrial dilation based on ASD size because external physiological variables confound the relationship. Understanding the relationship between ASD size and right atrium dilation would improve assessments of prognosis and treatment plans. This experiment quantifies the relationship between ASD size and right atrial dilation using an experimental model by measuring how the defect size affects right atrial fluid output. We hypothesized that larger ASDs result in greater, linearly increasing right atrium fluid output. We constructed the model using two fluid-filled chambers, scaled to represent the left and right atria, and simulated the ASD size by drilling incrementally larger openings between the chambers. In addition, we maintained fluid pressure separately, attuned to cardiovascular blood pressure, to mimic a realistic atrial setting. The findings support our hypothesis: across apertures of 6, 10, and 14 mm, right atrial fluid output increased with ASD diameter. These results provide a quantifiable relationship between ASD size and right atrial fluid output, presenting a cost-effective model to offer insight into ASD's effect on right atrial shunt, and inform clinical prognosis for ASD patients.**

## INTRODUCTION

The heart serves as the circulatory system's primary organ, pumping blood and other critical nutrients throughout the body (1). The human heart is composed of four chambers: the right and left atria, which form the upper chambers, and the right and left ventricles, which constitute the lower chambers (2). The right atrium collects deoxygenated blood returning from the body through the veins, whereas the left atrium receives oxygen-rich blood from the pulmonary veins (3). The muscle dividing the atria forms the septum (4). During fetal development, all babies have a normal opening in the septum called the foramen ovale, which allows blood to skip past the lungs as oxygenation occurs via the mother's placenta. Though this opening typically closes soon after birth, if it fails to close completely, the resulting opening is known as an atrial septal defect (ASD) (5). Over time, blood from the left atrium shunts to the right atrium because, under normal homeostatic conditions, the left atrium naturally has a higher blood pressure than the right atrium (6). Larger defect sizes cause significant increases in blood volume entering the right atrium, which responds by increasing contractile force to compensate for the extra load. However, prolonged increased volume causes the right atrium to stretch and dilate, forcing the right heart chambers to strain substantially (7). Eventually, excessive constriction causes cardiovascular muscles to dilate the right heart, which can lead to arrhythmia, pulmonary hypertension, and heart failure (8).

ASD is a common congenital heart defect worldwide, occurring in approximately one out of every thousand infants (9). Although larger defect sizes have life-threatening consequences, such as right-sided heart failure, symptoms for smaller defects range in severity from shortness of breath to increased risk of pneumonia and bronchitis (10). Since diagnosis requires acute attention to subtle murmurs from the heart, about a quarter of ASDs remain undiagnosed until adulthood, allowing long-term complications such as arrhythmia, pulmonary hypertension, and heart failure to develop (9, 11). This delay increases mortality rates to 1.7 times that of the general population (12).

Treatment options depend on defect size. Clinicians categorize ASDs by diameter into different categories, namely small (3-6 mm), moderate (6-12 mm), and large (>12 mm) (13). Doctors highly consider surgical intervention for larger defects, while smaller and moderate defects often remain untreated to allow the body to repair naturally (14, 15). Echocardiography is the primary diagnostic tool used to identify ASD size, with larger defects often being easier to detect due to more apparent blood flow issues, while smaller defects may require more sensitive imaging techniques such as cardiac MRI (16, 17).

Current work emphasizes treatment, including observation, symptom-directed medications, transcatheter closure, surgical repair, rather than quantifying physiological consequences (18, 19). To address this gap, we developed a physical model simulating atrial blood flow using two fluid-filled chambers representing the left and right atria. We represented ASD sizes with adjustable openings between the chambers and calibrated chamber pressures to match physiologic left-to-right pressure gradients. Our model relies on accessible materials, allowing other researchers to easily replicate and expand upon the design to create more anatomically accurate simulations and results. Using this setup, we aimed to define a quantifiable relationship between ASD size and right atrial (RA) fluid output, establishing a standardized trend to improve patient prognosis and guide clinical treatment. Since the flow rate through an opening is directly proportional to its cross-sectional area and the pressure gradient across it, we hypothesized that defect size would be linearly related to increases in RA fluid output (20).

https://doi.org/10.59720/25-056

Our results agree with this hypothesis, demonstrating that larger ASD sizes produced increased RA fluid output, which is consistent with the expected mechanism of RA dilation. These findings carry clinical implications by presenting a fundamental understanding of ASD prognosis based on defect severity. For patients with larger ASDs, these results provide a physiological basis for recommending surgical intervention. Conversely, for smaller ASDs, the linear relationship supports delaying immediate clinical intervention due to minimal right atrium dilation. Overall, this model offers a practical overview for understanding ASD prognosis and potentially guiding treatment plans for affected patients.

## RESULTS

There remains a gap in quantifying how specific ASD sizes translate into RA volume changes, since clinical data often confound size with other physiological variables (21). We hypothesized that larger ASD diameters would be associated with proportionally greater RA fluid output. To test this, we designed our model to reflect established patterns of left-to-right blood flow in ASDs (**Figure 1a**). We tested holes with 3 different diameters: 6 mm, 10 mm, and 14 mm, corresponding to small, medium, and large ASDs per standard prognosis categories, respectively (13). We also used a control group without connected tubing to represent a normal heart without an ASD and establish a baseline for comparison. We

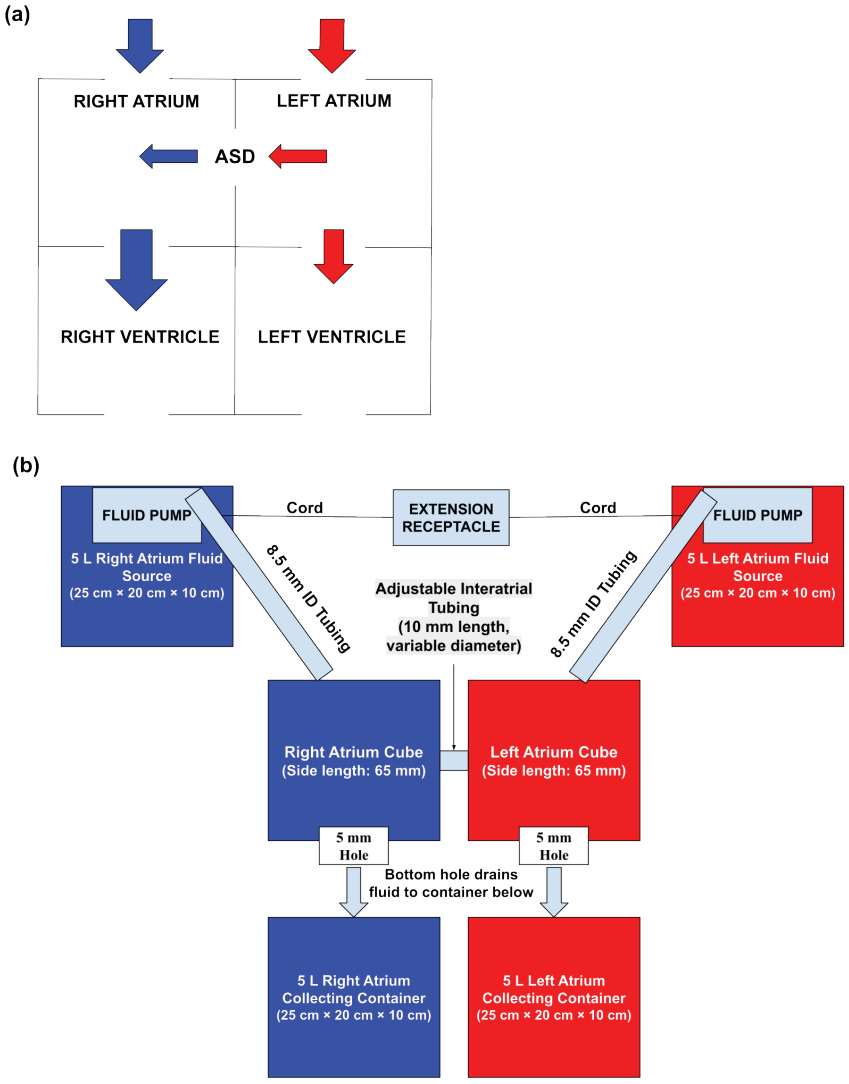


**Figure 1: Schematic of atrial septal defect (ASD) blood flow and experimental setup for modeling right atrial (RA) fluid output. (a)** Diagram of blood flow through an ASD, illustrating the left-to-right shunt from the left atrium to the right atrium due to higher left atrial pressure. **(b)** Diagram of the ASD model and dimensions. RA components are colored blue, left atrial components are colored red. Fluid pumps were powered via a switched extension receptacle. Adjustable-pressure pumps were submerged in a 5,000 $cm^3$ reservoir, and tubing delivered fluid at a fixed pressure to atrial containers positioned above. Three pairs of atrial cubes were used, each with a different interatrial tube diameter (6, 10, or 14 mm) to represent small, medium, and large defects. A 5 mm hole in the base of each atrium directed effluent into collection containers, which were weighed to calculate volume. Pumps were activated simultaneously for 5 s to measure right-atrial output; increases over the no-ASD control were interpreted as greater shunt magnitude. After each trial, both pumps were powered off and the midpoint clamp was closed to prevent post-run cross-flow.

https://doi.org/10.59720/25-056

measured RA fluid output across three trials per defect size to ensure consistency (**Figure 1b**).

Results demonstrated that increasing ASD diameter led to greater RA fluid output. We calculated increase in RA fluid output by subtracting the control group's output from that of each ASD size. The 6 mm, 10 mm, and 14 mm defect diameters produced average increases in RA fluid output of 2.33 mL, 5.67 mL, and 8.33 mL, respectively. We performed a linear regression to illustrate the relationship between ASD sizes and average increase in RA fluid output (**Figure 2**). As defect diameter increased, average RA fluid output increased proportionally, indicating a linear correlation (simple linear regression, $R^2$ = 0.9878, $p$ < 0.0001). The coefficient of determination ($R^2$ = 0.9878) demonstrates a strong fit between observed and expected values using the linear model, supporting the hypothesis of a linear relationship between ASD size and RA fluid output. Based on the regression model, for every millimeter of ASD size, we expected about 0.56 mL of increased RA fluid output.

To further evaluate whether the differences in fluid output between ASD size groups were statistically significant, we conducted a one-way Analysis of Variance (ANOVA) at a 5% significance level. The analysis showed a significant effect of ASD size on RA fluid output, supporting that increased ASD size leads to greater RA fluid output (ANOVA, F = 53.69, $p$ = 0.0000121).

## DISCUSSION

There is a lack of clear data on the relationship between ASD size and RA output, which our atrial model addresses by demonstrating that RA fluid output increases approximately linearly with ASD diameter. We hypothesized that the relationship between ASD size and RA fluid output would be a linear, direct relationship. By comparing the RA fluid output across different hole diameters, our results displayed a direct linear trend that confirmed the hypothesis. Recorded data aligned closely with the linear regression model. Further statistical analysis confirmed the hypothesis, showing that the results were statistically significant. Specifically, we expected RA fluid output to increase by about 0.56 mL for each millimeter of ASD size.

While an increase in RA fluid output serves as a strong indicator of the correlation between ASD size and RA dilation, the values themselves do not quantify the extent of dilation. For instance, an increase in 2.33 mL of RA fluid output does not equate to 2.33 mL enlargement of the right atrium itself. Nevertheless, the established linear relationship between ASD size and RA fluid output can be adopted as a reliable proxy to estimate RA dilation, as increased RA blood volume produces excessive pressure, which is the primary contributor to RA enlargement (9). Therefore, it is reasonable to conclude that larger ASDs are more likely to result in greater dilation. This is clinically relevant because RA dilation contributes to arrhythmias and right-sided heart failure, which underlie the symptoms observed in patients with ASD (11).

The direct correlation between ASD size and RA fluid output can be explained through hemodynamic principles, particularly the pressure gradient between the left and right atria. In a normal cardiovascular system, the left atrium operates at a slightly higher pressure than the right atrium (6). This difference in pressure contributes to a left-to-right shunt through the ASD, moving the blood from the left atrium into the right atrium, whereas no such shunt occurs in healthy hearts (7). Fluid dynamics expounds this linear relationship: the volumetric flow rate through an orifice is directly proportional to the orifice's cross-sectional area and the pressure gradient across it, assuming the discharge coefficient and fluid density are constant (20). As the flow rate into the right atrium through the ASD increases linearly based on the size of the defect, it explains the linear relationship between increase in RA fluid output and ASD diameter.

For output values from larger ASDs, there was a higher deviation from the mean compared to smaller defects. For example, the standard deviation for the 6 mm ASD size was 0.58 mL, while the standard deviation for the 14 mm ASD size was nearly triple this value (1.53 mL). We predicted

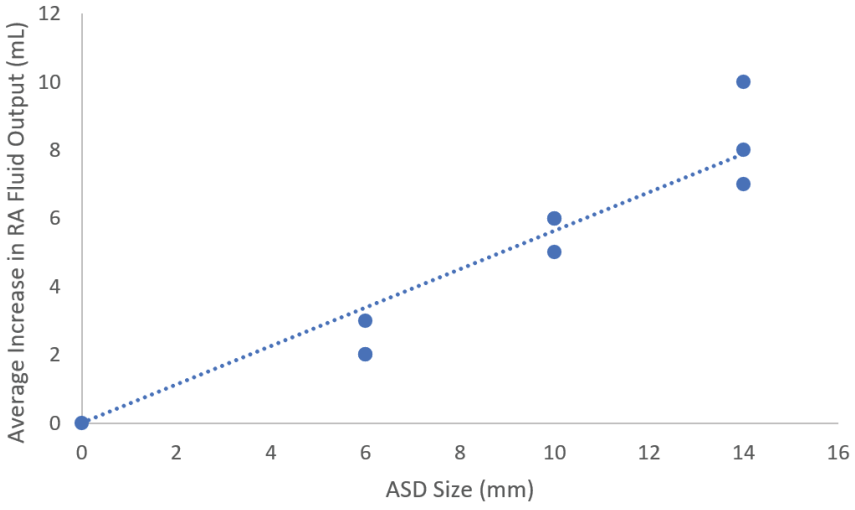


**Figure 2: Scatterplot comparing ASD size and RA fluid output.** The blue dotted line represents a simple linear regression model: average increase in RA fluid output = 0.5642x (ASD size). Coefficient of determination ($R^2$) = 0.9878, $p$ < 0.0001, F-ratio = 53.69, n = 3. Although three trials were performed for each ASD size, some points overlap on the plot because identical values were obtained: two 2 mL points for the 6 mm hole size and two 6 mL points for the 10 mm hole size.

https://doi.org/10.59720/25-056

that this variability was due to more pronounced fluctuations when working with greater flow rate from larger defect sizes. This meant that small changes in the system, such as inconsistencies with the fluid pump or time frame, had a much greater impact on the increase in RA fluid output in systems of larger ASDs. In contrast, for smaller ASD models, external factors would not have as significant an impact on the shunting of fluid between the atria, as reduced crossflow would reduce variability due to extrinsic effects.

Although our results provide insight into the extent of RA fluid output based on ASD size, due to a lack of funding and access to restricted tools, our model itself is limited in its ability to replicate many physiological cardiovascular elements. Due to resource constraints, only these three diameters were modeled, which may limit the generalizability of our findings. Additionally, because a 1:1 model would make observation and adjustment of atrial components unfeasible, all components were scaled by five. Although scaling the model should not have changed the type of relationship hypothesized in the experimental question, it likely resulted in an overestimation of the absolute RA flow for a given ASD diameter, because the rigid, oversized chamber lacked physiologic compliance and valve dynamics that would combat shunt over time. In addition, the structural form of the atrial chambers poses a challenge in accurately replicating cardiovascular conditions, as the atrium, although approximately cuboidal, includes an auricle extension that partially affects the left-to-right shunt (22). In our model, the flow of fluid was uniform and directed more directly toward the center of the atrium (23). However, the ear-shaped auricle creates a distinct structural intrusion that alters the uniformity of circulation, changing the direction of flow that overestimate RA outflow by reducing recirculation-related energy losses (24). Furthermore, our model's representation of cardiovascular valves as unchanging holes at the bottom of each atria oversimplified the role of valves in RA dilation. In the right atrium, the base hole represents the tricuspid valve, which opens and closes to prevent blood from flowing in the wrong direction (25). Nevertheless, results from our model should still offer valuable insights into RA fluid output, as the observed statistical significance reflects trends within the model, even if the measurements may not directly match those of an actual heart. Our model also remained rigid and at a constant shape throughout the experiment, which is different to how the atrium repeatedly expands and contracts under pressure, possibly changing the relevance in the experimental data (26). Though these are the limitations in replicating the cardiovascular system that are majorly relevant to RA dilation, differences exist in our model unrelated to the experimental question.

As mentioned previously, further research could improve the existing model by replicating cardiovascular elements more accurately. Newer models could implement pulsatile flow to simulate the cardiac cycle's systolic and diastolic phases, and employ atrial shape and dynamic valves to increase physiological relevance. Additional studies could also expand the scope of pathophysiological understanding by investigating the impact of ASDs in different physiological or pathological states. For example, to study age-related changes with differing average blood pressures, models could be adjusted to simulate differences in atrial compliance and flow patterns between pediatric and adult populations. Using the ASD model, further research could explore the effectiveness of different medical interventions. By using a variety of treatments, such as device closure techniques and pharmacological interventions, analyzing the RA fluid output for each intervention could determine the best treatment option.

To apply the findings from this study into clinical settings, several key steps should be taken to confirm its efficacy. First, our model should be validated against real-world data by comparing its results with clinical observations and outcomes in patients with ASD. Researchers should collaborate with healthcare institutions to gather patient data and use it to confirm our model's predictions. Additionally, in vivo studies should be conducted using pig heart models that are similar in structure and physiology to the human heart to provide insights into how atrial dilation is affected by ASD size under dynamic, biologically accurate conditions (27). Improving the existing model by replicating cardiovascular conditions more accurately, such as by introducing pulsatile flow or compliant structures, should also be done to refine its medical accuracy (28, 29). Once finalized and validated, our model has the potential to fill gaps in understanding the physiological effects of varying ASDs, ultimately improving patient outcomes by guiding more informed and precise clinical decisions.

Regardless of limitations, our model still holds clinical significance by providing a simplified yet effective framework for understanding the physiological effects of ASD. By recording RA fluid output for standardized defect severities, the study identifies a linear trend between defect size and RA fluid output that may be used to inform clinical decisions in conjunction with other clinical assessments. Because our model is cost-effective and accessible in design, it offers a foundational approach to exploring key aspects of ASD pathophysiology, offering a basis to further studies that utilize more advanced and costly simulations/clinical studies. In addition, this study provides insight into a gap in scientific research by offering one approach to relate ASD size to prognosis, which although is clinically relevant, has been relatively unaddressed up to now. Despite simplifying some cardiovascular components, our results do yield significant insights that highlight our model's significance as a research tool and a starting point for developing knowledge about ASDs in clinical contexts.

## MATERIALS AND METHODS

### Experimental Setup and Methodology

Cube containers modeling the atriums were constructed using 65 mm small acrylic boxes (Ganydet, Cat# B09HBZNC43). Four pairs of atrial cubes were utilized to test the three defect sizes (6 mm, 10 mm, 14 mm) and the control model. To allow for easier observation and manipulation, atrial cubes and the septum in our model were scaled by a factor of five. For this reason, each atrium was represented by a 65 mm cube, yielding a volume of approximately 274.6 mL (274,625 $mm^3$), which is five times the average adult RA volume of around 55 mL (30). The left and right atria were modeled using identical cubes, as both atria are roughly equal in volume under normal physiological conditions (31). Clear acrylic boxes were chosen for their durability, transparency, and ease of modification, such as drilling to insert tubing (**Figure 1b**).

To simulate varying sizes of ASDs, a hole was drilled at the center of one side of the three pairs of atrial cubes were

https://doi.org/10.59720/25-056

drilled. These holes had diameters of either 6 mm, 10 mm, and 14 mm, respectively. These holes were connected by silicone rubber tubes (QJZXUEZHEN, Cat# B08GPBC7C6) with corresponding diameters. The connecting tube between atrial cubes was cut to a length of 10 mm using a handsaw, then securely fitted and sealed with adhesive tape into the side holes of each cube. This length reflects the average adult atrial septum length of 2 mm, scaled up by a factor of five (32). For the control model without ASD, the atrial cubes were left unconnected without drilling holes at the side of both atriums.

A cordless drill (RYOBI, Cat# B0BSHXXVQD) was used to bore 5 mm holes at the bottom of each acrylic box for atrial fluid to be expelled and recorded. The 5 mm holes at the base of each atrial cube were not intended to replicate the mitral and tricuspid valves. Instead, they served a purely functional purpose: to provide an outlet for fluid to exit the chambers and be measured. For this reason, the holes at the base of each atrial cube were not scaled or designed to replicate the anatomical dimensions of the mitral or tricuspid valves.

To set up the atrial fluid source, two 5 L bowls were each filled with 4 L of tap water and placed side by side, half a meter behind the atrial cubes. The receiving front of the fluid pumps (CWKJ, Cat# B07SGMNKRP) was attached to the base of each bowl, with the ends of each tube positioned vertically above their corresponding atrial cube, pointing straight downward. The fluid pump for the right atrium was set to a pressure of 530 Pa (~4 mmHg), while the pump for the left atrium was set to a pressure of 2000 Pa (~15 mmHg), which matches the atrial pressure of both atriums (33). The silicone tubes connected to each fluid pump were shortened to 25 cm to prevent excessive length, which could cause the tubes to coil unnecessarily. Identical 5 L collecting containers were placed underneath the hole drilled at the bottom of each atrial cube to collect the fluid output from both sides. A digital scale was prepared to convert the mass of each collecting container into milliliters for accurate data collection at the end of each trial. A digital stopwatch was also used to time each simulation.

### Simulation Process

Atrial cube pairs were each positioned above the collecting containers one at a time. The digital stopwatch and fluid pump were then activated simultaneously. After five seconds, the pump was turned off. We selected five seconds for the run-time of each simulation as it allowed sufficient fluid displacement while preventing overflow from the atrial cubes. At the end of each trial, a mini tube clamp (Sioux Chief, Cat# B09RMSZ785) was engaged at the midpoint of the interatrial connector to prevent cross-atrial flow beyond the experimental time frame. The collecting container for the right atrial cube was weighed on the digital scale to determine RA fluid output. Dimensional analysis was used to convert the output fluid from grams to milliliters, which was then recorded as data for analysis. Each control/ASD model was simulated three times to ensure an accurate result. After every trial, the model was reset to its original experimental setup by cleaning the modeled atriums and collecting containers, refilling the fluid source, recalibrating the scale and timer.

### Statistical Analysis

For each ASD size, we calculated the averages for increase in RA fluid output. We then created a scatterplot in Excel to visualize the data and performed statistical analysis in Python (version 3.11) using the statsmodels package (version 0.14.0) (34). This included constructing a linear regression model to determine if the relationship between ASD size and RA fluid output confirmed the hypothesis, calculating standard deviations for each defect size, obtaining *p*-values to assess statistical significance, and conducting a one-way ANOVA at a 5% significance level with the corresponding F-ratio. To determine if our results closely aligned with the linear regression model, we calculated the coefficient of determination.

**Received:** February 5, 2025
**Accepted:** July 7, 2025
**Published:** December 6, 2025

## REFERENCES

1. Cleveland Clinic. "Heart." *Cleveland Clinic*, https://my.clevelandclinic.org/health/body/21704-heart. Accessed 16 June 2025.
2. Michigan Medicine. "Anatomy of the Human Heart." *Michigan Medicine*, https://www.michiganmedicine.org/health-lab/anatomy-human-heart. Accessed 16 June 2025.
3. MedlinePlus. "Heart Chambers." *MedlinePlus*, https://www.medlineplus.gov/ency/imagepages/19612.htm. Accessed 16 June 2025.
4. Texas Heart Institute. "Heart Anatomy." *Texas Heart Institute*, https://www.texasheart.org/heart-health/heart-information-center/topics/heart-anatomy/. Accessed 16 June 2025.
5. Nemours KidsHealth. "Patent Foramen Ovale (PFO)." *KidsHealth*, https://www.kidshealth.org/en/parents/pfo.html. Accessed 16 June 2025.
6. Dehn, Anna Maria, *et al.* "Atrial Septal Defect: Larger Right Ventricular Dimensions and Atrial Volumes as Early as in the First Month After Birth—A Case-Control Study Including 716 Neonates." *Pediatric Cardiology*, vol. 44, no. 7, Oct. 2023, https://doi.org/10.1007/s00246-023-03211-z.
7. Merck Manual Professional Edition. "Atrial Septal Defect (ASD)." *Merck Manuals: Professional Edition*, https://www.merckmanuals.com/professional/pediatrics/congenital-cardiovascular-anomalies/atrial-septal-defect-asd. Accessed 16 June 2025.
8. Mayo Clinic Staff. "Atrial Septal Defect (ASD) — Symptoms and Causes." *Mayo Clinic*, https://www.mayoclinic.org/diseases-conditions/atrial-septal-defect/symptoms-causes/syc-20369715. Accessed 16 June 2025.
9. Centers for Disease Control and Prevention. "About Atrial Septal Defect (ASD)." *CDC*, https://www.cdc.gov/heart-defects/about/atrial-septal-defect.html. Accessed 16 June 2025.
10. Yale Medicine. "Atrial Septal Defect (ASD)." *Yale Medicine*, https://www.yalemedicine.org/conditions/atrial-septal-defect-asd. Accessed 16 June 2025.
11. Sinan, Umit Yasar, *et al.* "Long-term follow-up results of adult atrial septal defect population." *BMC Cardiovascular Disorders*, vol. 25, no. 1, Aug. 2025, https://doi.org/10.1186/s12872-025-05095-8.
12. Nyboe, Camilla, *et al.* "Long-term mortality in patients with atrial septal defect: A nationwide cohort-study." *European*

https://doi.org/10.59720/25-056

*Heart Journal*, vol. 39, no. 12, Dec. 2017, pp. 993–998, https://doi.org/10.1093/eurheartj/ehx687.
13. McMahon, Colin J., *et al.* "Natural History of Growth of Secundum Atrial Septal Defects and Implications for Transcatheter Closure." *Heart*, vol. 87, no. 3, 2002, pp. 256–59, https://doi.org/10.1136/heart.87.3.256.
14. MedlinePlus. "Atrial Septal Defect (ASD)." *MedlinePlus*, https://www.medlineplus.gov/ency/article/000157.htm. Accessed 16 June 2025.
15. UCSF Health. "Minimally Invasive Closure of Atrial Septal Defect." *UCSF Health*, https://www.ucsfhealth.org/treatments/minimally-invasive-closure-of-atrial-septal-defect. Accessed 16 June 2025.
16. Lin, Xixiang, *et al.* "Echocardiography-Based AI for Detection and Quantification of Atrial Septal Defect." *Frontiers in Cardiovascular Medicine*, vol. 10, 2023, https://doi.org/10.3389/fcvm.2023.985657.
17. Mayo Clinic Staff. "Atrial Septal Defect (ASD) — Diagnosis and Treatment." *Mayo Clinic*, https://www.mayoclinic.org/diseases-conditions/atrial-septal-defect/diagnosis-treatment/drc-20369720. Accessed 16 June 2025.
18. Brida, Margarita, *et al.* "Atrial Septal Defect in Adulthood: A New Paradigm for Congenital Heart Disease." *European Heart Journal*, vol. 43, no. 28, 21 July 2022, pp. 2660–2671, https://doi.org/10.1093/eurheartj/ehab646.
19. Baumgartner, Helmut, *et al.* "2020 ESC Guidelines for the Management of Adult Congenital Heart Disease: The Task Force for the Management of Adult Congenital Heart Disease of the European Society of Cardiology (ESC). Endorsed by: Association for European Paediatric and Congenital Cardiology (AEPC), International Society for Adult Congenital Heart Disease (ISACHD)." *European Heart Journal*, vol. 42, no. 6, 7 Feb. 2021, pp. 563–645, https://doi.org/10.1093/eurheartj/ehaa554
20. University of Texas. "Flow Through an Orifice." *University of Texas*, https://farside.ph.utexas.edu/teaching/336L/Fluidhtml/node55.html. Accessed 16 June 2025.
21. Zaragoza-Macias, E., *et al.* "Interventional Therapy Versus Medical Therapy for Secundum Atrial Septal Defect: A Systematic Review (Part 2) for the 2018 AHA/ACC Guideline for the Management of Adults With Congenital Heart Disease." *Journal of the American College of Cardiology*, vol. 73, no. 12, Apr. 2019, pp. 1579–1595, https://doi.org/10.1016/j.jacc.2018.08.1032.
22. Elsevier. "Right Auricle of Heart." *Elsevier Anatomy Resources*, https://www.elsevier.com/resources/anatomy/cardiovascular-system/heart-pericardium/right-auricle-of-heart/20454. Accessed 16 June 2025.
23. University of Groningen. "Vector Visualization." *Data Visualization Book*, https://www.cs.rug.nl/svcg/DataVisualizationBook/Sp6. Accessed 16 June 2025.
24. Veer Surendra Sai University of Technology. *Fluid Mechanics Lecture Notes*, https://www.vssut.ac.in/lecture_notes/lecture1525499954.pdf. Accessed 16 June 2025.
25. Cleveland Clinic. "Tricuspid Valve." *Cleveland Clinic*, https://my.clevelandclinic.org/health/body/21851-tricuspid-valve. Accessed 16 June 2025.
26. Marino, Paolo N., *et al.* "Complex Interaction between the Atrium and the Ventricular Filling Process: The Role of Conduit." *Open Heart*, vol. 6, no. 2, 2019, e001042, https://doi.org/10.1136/openhrt-2019-001042.
27. Lunney, Joan K., *et al.* "Importance of the pig as a human biomedical model." *Science Translational Medicine*, vol. 13, no. 621, Nov. 2021, https://doi.org/10.1126/scitranslmed.abd5758.
28. Gerrah, Rabin, and Stephen J. Haller. "Computational Fluid Dynamics: A Primer for Congenital Heart Disease Clinicians." *Asian Cardiovascular and Thoracic Annals*, vol. 28, no. 8, 2020, pp. 520–532, https://doi.org/10.1177/0218492320957163.
29. Pennati, G., F. Migliavacca, G. Dubini, *et al.* "Use of Mathematical Model to Predict Hemodynamics in Cavopulmonary Anastomosis with Persistent Forward Flow." *Journal of Surgical Research*, vol. 89, 2000, pp. 43–52, https://doi.org/10.1006/jsre.1999.5799.
30. Sun, Zhen-Yun, *et al.* "Echocardiographic Evaluation of the Right Atrial Size and Function: Relevance for Clinical Practice." *American Heart Journal Plus: Cardiology Research and Practice*, vol. 27, 2023, 100274, https://doi.org/10.1016/j.ahjo.2023.100274.
31. The Common Vein. "Right Atrium Size." *The Common Vein*, https://www.thecommonvein.com/heart/right-atrium-size. Accessed 16 June 2025.
32. The Common Vein. "Atrial Septum Size." *The Common Vein*, https://www.thecommonvein.com/heart/atrial-septum-size. Accessed 16 June 2025.
33. Ragosta, Michael. "Normal Waveforms, Artifacts, and Pitfalls." *Textbook of Clinical Hemodynamics*, W.B. Saunders, 2008, pp. 16–37.
34. Seabold, Skipper, and Josef Perktold. "Statsmodels: Econometric and Statistical Modeling with Python." *Proceedings of the 9th Python in Science Conference*, edited by Stéfan van der Walt and Jarrod Millman, 2010, pp. 92–96, https://doi.org/10.25080/Majora-92bf1922-011.